2013

UV and Visible Light Activated TiO2 Photocatalysis of 6-Hydroxymethyluracil, a Model Compound for the Potent Cyanotoxin Cylindrospermopsin

Cen Zhao
Florida International University

Miquel Pelaez
University of Cincinnati,

Dionysios Dionysiou
University of Cincinnati,

See next page for additional authors

Recommended Citation

Zhao, C. et al. (2013) UV and visible light activated TiO2 photocatalysis of 6-hydroxymethyluracil, a model compound for the potent cyanotoxin cylindrospermopsin. *Catalysis Today,* Vol. 224, April 2014. Available online October, 2013. doi:10.1016/j.cattod.2013.09.042

Catalysis Today xxx (2013) xxx–xxx

Contents lists available at ScienceDirect

Catalysis Today

journal homepage: www.elsevier.com/locate/cattod

UV and visible light activated TiO_2 photocatalysis of 6-hydroxymethyl uracil, a model compound for the potent cyanotoxin cylindrospermopsin

Cen Zhao [a], Miguel Pelaez [b], Dionysios D. Dionysiou [b], Suresh C. Pillai [c], John A. Byrne [d], Kevin E. O'Shea [a,*]

[a] Department of Chemistry and Biochemistry, Florida International University, Miami, FL 33199, USA
[b] Environmental Engineering and Science Program, University of Cincinnati, Cincinnati, OH 45221-0012, USA
[c] Centre for Research in Engineering Surface Technology (CREST), Focas Institute, Dublin Institute of Technology, Kevin Street, Dublin 8, Ireland
[d] Nanotechnology Integrated Bio-Engineering Centre, University of Ulster, Newtownabbey, Northern Ireland BT37 0QB, UK

ARTICLE INFO

Article history:
Received 2 August 2013
Received in revised form
11 September 2013
Accepted 22 September 2013
Available online xxx

Keywords:
Cylindrospermopsin (CYN)
6-Hydroxymethyl uracil (6-HOMU)
NF-TiO_2
Photocatalysis
Visible light

ABSTRACT

TiO_2 photocatalyses of 6-hydroxymethyl uracil (6-HOMU) a model compound for the potent cyanotoxin, cylindrospermopsin (CYN), were carried out employing visible and UV irradiation using different non-metal doped TiO_2 materials, nitrogen and fluorine-TiO_2 (NF-TiO_2), phosphorus and fluorine-TiO_2 (PF-TiO_2) and sulfur-TiO_2 (S-TiO_2). The model compound was readily degraded under UV TiO_2 photocatalysis with pseudo-first-order rate constants (k) of 2.1, 1.0, and 0.44 h^{-1} for NF-TiO_2, PF-TiO_2 and S-TiO_2, respectively. Under visible light activated (VLA), NF-TiO_2 was the most active photocatalyst, PF-TiO_2 was marginally active and S-TiO_2 inactive. VLA NF-TiO_2 was effective and increased the k with increasing pH from 3 to 9. The presence of humic acid (HA), Fe^{3+} and Cu^{2+} can enhance the degradation. However, at 20 ppm HA significant inhibition was observed, likely due to shadowing of the catalyst, quenching of ROS or blocking active sites of TiO_2. We probed the roles of different reactive oxygen species (ROS) using specific scavengers and the results indicate that $O_2^{\bullet -}$ plays an important role in VLA TiO_2 photocatalysis. Our results demonstrate that NF-TiO_2 photocatalysis is effective under UV and visible irradiation and over a range of water qualities. VLA NF-TiO_2 photocatalysis is an attractive alternative technology for the CYN contaminated water treatment.

1. Introduction

Cyanobacteria commonly exist in drinking water sources and can lead to harmful algae blooms (HABs). Seventy percent of HABs can produce potent toxins [1,2] and thus pose a tremendous risk to humans and the environment. One of the more problematic cyanotoxins is cylindrospermopsin (CYN), an alkaloid with a tricyclic guanidine group and uracil ring. CYN has been showed to be genotoxic [3,4] and carcinogenic [5]. The main target organs of CYN include the liver, kidney, thymus, lungs and adrenal glands. Human exposure to cylindrospermopsin occurs through ingestion of CYN contaminated food or water, or during recreational activities during HABs in lakes and fresh water systems. The most notable incident of CYN on human health occurred on Palm Island, Australia in 1979, which led to hepatoenteritis in 138 children and 10 adults [6]. Despite this notorious incident, CYN was not isolated and identified until 1992 [7]. CYN is also responsible for the poisoning of livestock [8].

The occurrences and volumes of toxic cyanobacterial blooms have increased significantly in recent years due to climate change and increasing eutrophication. With the increasing pressure and global need for clean water, it is desirable to identify a sustainable treatment process for the elimination of naturally occurring cyanotoxins from drinking water. Conventional water treatment methods such as coagulation, flocculation, sedimentation and filtration are often not viable for removing cyanotoxins [9,10]. Although activated carbon may be effective to remove cyanotoxins in the laboratory, treatments of large volumes of contaminated water are often not economically practical. The high levels of natural organic material (NOM) associated with HABs can have a pronounced negative impact on the effectiveness of the activated carbon process [11]. Chlorine and ozone based treatments have been studied for removal of cyanotoxins, however, by products like trihalomethanes (THMs) (by chlorination) and bromate (by ozonation) are a concern because of associated health consequences [12,13].

* Corresponding author. Tel.: +1 305 348 3968; fax: +1 305 348 3772.
E-mail address: osheak@fiu.edu (K.E. O'Shea).

0920-5861/$ – see front matter © 2013 Elsevier B.V. All rights reserved.
http://dx.doi.org/10.1016/j.cattod.2013.09.042

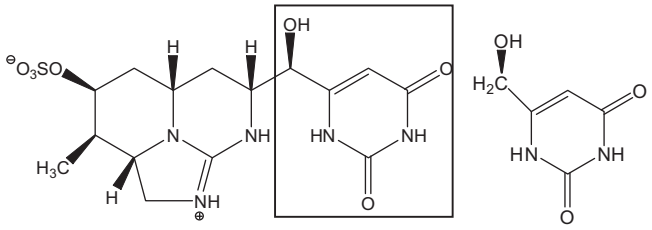

Fig. 1. Structure of cylindrospermopsin (CYN) and the model compound 6-hydroxymethyl uracil (6-HOMU).

Advanced oxidation processes (AOPs) have received considerable attention for the treatment of water contaminated with a wide variety of toxins and pollutants. AOPs employ the hydroxyl radical ($HO^{\bullet}$) as the primary oxidant in the oxidative remediation of toxins in drinking water. $HO^{\bullet}$ is a very powerful oxidant, which can react rapidly with nearly all organic compounds due to its strong oxidation potential (+2.80 V) [14]. UV TiO_2 photocatalysis is effective for the destruction of an extensive number of toxins and organic contaminants in the wastewater and drinking water [15,16]. Conventional UV TiO_2 photocatalysis can produce a number of reactive oxygen species (ROS), however $HO^{\bullet}$ is generally associated with the effective destruction of organic compounds. UV photoexcitation of TiO_2 produces electron/hole (e_{cb}^-/h_{vb}^+) pairs as illustrated by Eq. (1). The e_{cb}^- can reduce molecular oxygen yielding superoxide anion radical ($O_2^{\bullet -}$), Eq. (2) and the h_{vb}^+ has the potential to oxidize surface absorbed H_2O or hydroxyl groups to generate $HO^{\bullet}$, Eq. (3). Another source of $HO^{\bullet}$ can occurs via disproportionation of $O_2^{\bullet -}$, yielding H_2O_2, Eq. (4), which can be reduced to $HO^{\bullet}$ Eq. (5).

$$TiO_2 + h\nu \rightarrow e_{cb}^- + h_{vb}^+ \quad (1)$$

$$e_{cb}^- + O_2 \rightarrow O_2^{\bullet -} \quad (2)$$

$$h_{vb}^+ + H_2O \rightarrow H^+ + HO^{\bullet} \quad (3)$$

$$2O_2^{\bullet -} + 2H_2O \rightarrow H_2O_2 + 2OH^- + O_2 \quad (4)$$

$$H_2O_2 + e_{cb}^- \rightarrow OH^- + HO^{\bullet} \quad (5)$$

Limitations effecting the broad application of UV TiO_2 photocatalysis include the requirement of costly UV light (<387 nm) and the rapid recombination of e_{cb}^-/h_{vb}^+ pairs, leading to low quantum yields. The wavelengths of solar irradiation that reach the surface of the earth are mostly in the visible region (40%) with a small fraction (5%) in UV region. Hence, photocatalysts activated by visible light or by a broad spectrum of wavelengths (solar) have significant economic advantages. Doping of TiO_2 (NF-TiO_2, PF-TiO_2 and S-TiO_2) can result in a decrease band gap such that longer wavelength light (visible and solar light) becomes applicable [17,18]. In addition, doped TiO_2 can inhibit e_{cb}^-/h_{vb}^+ pairs recombination through trapping of charge carriers. VLA photocatalysis employing TiO_2 based materials has received significant attention recently and also been reviewed by the research groups of Zhao [19] and Dionysiou [20]. UV and VLA TiO_2 photocatalysis are effective for treatment of microcystin cyanotoxins (MC), however only a limited number of reports have appeared on the photocatalysis of CYN [21]. The high cost of CYN limited our ability to conduct detailed studies to optimize the reaction conditions for the TiO_2 photocatalytic destruction of CYN. The uracil moiety in CYN is critical to the toxicity of CYN. $HO^{\bullet}$ reacts primarily (84%) at the uracil ring of CYN [22]. With this in mind, 6-hydroxymethyl uracil (6-HOMU) (Fig. 1) was synthesized and used as a model compound for the UV and VLA photocatalysis of CYN. We report herein the photocatalytic activity of different non-metal doped TiO_2 materials, NF-TiO_2, PF-TiO_2 and S-TiO_2 under 350, 420 and 450 nm irradiation. Among these photocatalysts, NF-TiO_2 was the most UV and visible light active for the degradation of the CYN model compound. The treatment is effective over a range of pH, and in the presence of ions and HA. $O_2^{\bullet -}$ appears to play the predominant role in the VLA photocatalytic degradation process. Our results demonstrate NF-TiO_2 can be used for the UV and visible light photocatalytic destruction of uracil based compounds under a variety of conditions.

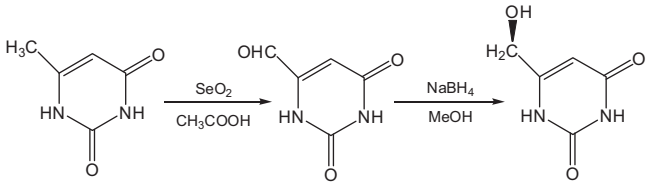

Fig. 2. Synthesis of 6-hydroxymethyl uracil.

2. Materials and methods

2.1. Materials

$FeCl_3{\cdot}6H_2O$, $CuCl_2{\cdot}2H_2O$, $CaCl_2{\cdot}2H_2O$, $MgCl_2$ as the sources of common ions, acetic acid, sodium bisulfite and HPLC grade methanol were purchased from Fisher Scientific. The humic acid was obtained from Fluka. 6-Methyl uracil and selenium dioxide were purchased from Sigma Aldrich. Sodium borohydride was obtained from Acros organics. All reagents were used as received. The synthesis and characterization of the doped-TiO_2 materials (NF-TiO_2, PF-TiO_2, and S-TiO_2) are reported elsewhere [17,18]. The model compound (6-hydroxymethyl uracil) was synthesized according to standard organic functional group transformations. All aqueous solutions were prepared with Millipore filtered water.

2.2. Sample preparation

The loading of doped-TiO_2 materials employed for UV photocatalysis experiments was 0.05 g/L with the initial model compound concentration of 5 ppm unless otherwise stated. VLA TiO_2 photocatalysis of model compound was conducted with 0.1 g/L NF-TiO_2 and 1 ppm initial concentration of model compound. The reaction solution was transferred to a pyrex cylindrical reactor (12 × 1 in., 150 mL capacity, with a vented Teflon screw top) and magnetically stirred in the dark and purged with oxygen for 15 min prior to irradiation and during irradiation. A Rayonet photochemical reactor (Southern New England Ultra Violet Company, www.rayonet.org, model RPR-100) was used for all experiments, equipped with a cooling fan and 15 phosphor-coated inter changeable lamps at λ = 350, 420 and 450 nm. Aliquots (1 mL) were collected at given time intervals and filtered through a 0.45 μm filter prior to high-performance liquid chromatography (HPLC) analysis.

2.3. Preparation of model compound

The synthesis of 6-HOMU includes two steps (Fig. 2): synthesis of orotaldehyde and reduction of orotaldehyde to 6-HOMU. The orotaldehyde was prepared by Kwang-Yuen's method [23]. Briefly, 6-methyl uracil (2.54 g) was refluxed in acetic acid (60 mL) with selenium dioxide (2.66 g) for 6 h. The hot reaction mixture was filtered and the yellow filtrate collected and solvent evaporated. The crude orotaldehyde was then dissolved in hot water (24 mL) and 5% sodium bisulfite was added dropwise into the stirred mixture. The solution was boiled with active carbon for 10 min and then gravity filtered to remove the carbon. The filtrate was acidified to

Please cite this article in press as: C. Zhao, et al., UV and visible light activated TiO_2 photocatalysis of 6-hydroxymethyl uracil, a model compound for the potent cyanotoxin cylindrospermopsin, Catal. Today (2013), http://dx.doi.org/10.1016/j.cattod.2013.09.042

Table 1
Doped TiO_2 band gaps and corresponding photoexcited wavelengths.

Doped TiO_2	Band-gap (eV)	Wavelength λ (nm)
S-TiO_2	2.94 [18]	422
NF-TiO_2	2.75 [17]	451
PF-TiO_2	2.68	463

pH 1 using concentrated HCl. Upon cooling, pure orotaldehyde was obtained as a precipitate from the solution. A mixture of pure orotaldehyde (0.14 g) and sodium borohydride (0.076 g) was refluxed in 95% methanol for 4 h. The resulting solution was filtered and the solvent was evaporated yielding the pure 6-HOMU with the purity of 98%. ^{1}H NMR spectrum (400 MHz, D_2O): δ 4.234 (2H, s, CH_2), 5.679 (1H, s, H5). ^{13}C NMR (400 MHz, D_2O): δ 62.18 (CH_2), 98.76 (C5), 160.19 (C2), 167.86 (C6), 170.63 (C4). Mass spectrum (ESI): m/z 141.1 (M−1).

2.4. Analysis

The concentration of the model compound was monitored by HPLC, Varian ProStar equipped with a ProStar 410 autosampler and a ProStar 335 photodiode array detector under the following conditions: a Luna RP C18 column (5 μm, 250 mm × 4.6 mm); 30 μL injection volume and 1 mL/min flow rate; The mobile phase was consisted of a linear gradient starting at 5% methanol, 95% water increased to 30% methanol in 5 min and then held constant for an additional 5 min; the detection wavelength was at 260 nm.

3. Results and discussion

3.1. TiO_2 photocatalysis of 6-hydroxymethyl uracil

TiO_2 photocatalysis experiments were carried out with 6-HOMU under 350, 420 and 450 nm irradiation varying only the catalysts, NF-TiO_2, PF-TiO_2 and S-TiO_2, to evaluate the relative photocatalytic activity of these non-metal doped TiO_2 materials. The concentration of 6-HOMU was monitored by HPLC as a function of irradiation time (Fig. 3). Under UV irradiation (350 nm), the degradation follows the order of NF-TiO_2 > PF-TiO_2 > S-TiO_2. The percent removal of 6-HOMU was 100, 86 and 59% for NF-TiO_2, PF-TiO_2 and S-TiO_2, respectively after 120 min of UV irradiation. The observed pseudo-first-order rate constants (k) were 2.1 h^{-1} for NF-TiO_2, 1.0 h^{-1} for PF-TiO_2, and 0.44 h^{-1} for S-TiO_2. VLA NF-TiO_2 photocatalysis (at 420 and 450 nm) leads to the degradation of 6-HOMU but at a slower rate than under UV irradiation (Fig. 3). 6-HOMU was slightly degraded by PF-TiO_2 under 420 nm irradiation and no degradation was observed employing S-TiO_2 under our VLA (450 nm) conditions. The photocatalytic activity of these materials is dependent on the recombination e_{cb}^-/h_{vb}^+ pairs, the band gap energies and structural properties [17]. The band gaps of NF-TiO_2, PF-TiO_2 and S-TiO_2 and the corresponding photoexcitation wavelengths are presented in Table 1.

PF-TiO_2 has the smallest band gap and should be activated by wavelengths of ≤463 nm. However, no degradation was observed at 450 nm during VLA PF-TiO_2 under our conditions, indicating that PF-TiO_2 has the poor photocatalytic activity likely due to faster recombination e_{cb}^-/h_{vb}^+ pairs and poor structural properties. While the band gap energy of S-TiO_2 (~422 nm) matches well with the light source of 420 nm, no detectable degradation of 6-HOMU was observed under 420 nm irradiation after 4 h. VLA S-TiO_2 photocatalysis was reported to be effective for the destruction of microcystin-LR (MC-LR) [18]. The differences in the structures

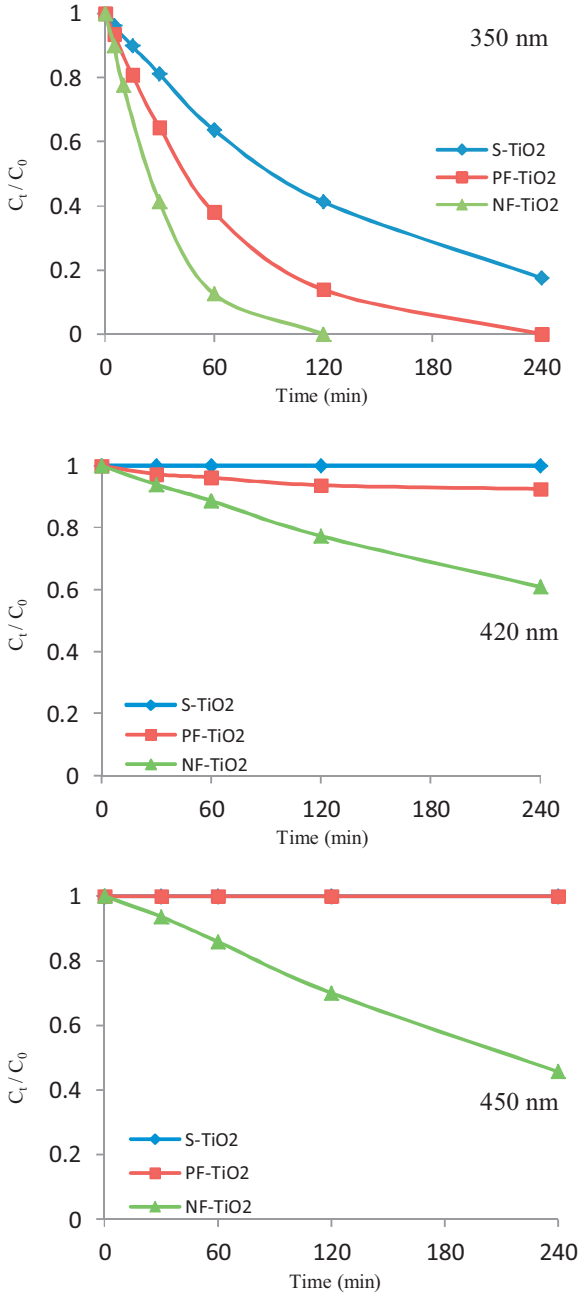

Fig. 3. TiO_2 photocatalysis of 6-HOMU under 350, 420 and 450 nm. [6-HOMU]$_0$ = 5 ppm, [TiO_2] = 0.05 g/L. The reproducibility is within ±10% on the basis of triplicate runs.

of the MC-LR and 6-HOMU will influence the adsorption and hence degradation of these compounds. MC-LR has more functional groups (carboxylic acid, amide, amine) than 6-HOMU, which will enhance the adsorption and subsequent degradation of MC-LR by the surface initiated processes involved in heterogeneous photocatalysis. NF-TiO_2 leads to the effective degradation of 6-HOMU under UV and visible light irradiation indicating the recombination of e_{cb}^-/h_{vb}^+ pairs in NF-TiO_2 with a band gap of 2.75 eV is slow enough to allow the production of ROS [17]. VLA TiO_2 photocatalysis using NF-TiO_2 is reported to be effective for a number of compounds including acetic acid [24] and 4-chlorophenol [25]. Our results indicate that NF-TiO_2 should be an effective visible light driven photocatalyst for the destruction of the CYN.

Please cite this article in press as: C. Zhao, et al., UV and visible light activated TiO_2 photocatalysis of 6-hydroxymethyl uracil, a model compound for the potent cyanotoxin cylindrospermopsin, Catal. Today (2013), http://dx.doi.org/10.1016/j.cattod.2013.09.042

Table 2
Pseudo-first-order rate constants (k) of 6-HOMU under 350, 420 and 450 nm irradiation.

Photocatalysts	k (h^{-1}) (R^2)		
	350 nm	420 nm	450 nm
S-TiO_2	0.44 (0.999)	0.0 (1.00)	0.0 (1.00)
PF-TiO_2	1.0 (0.999)	0.03 (0.915)	0.0 (1.00)
NF-TiO_2	2.1 (0.994)	0.12 (0.994)	0.20 (0.996)

3.2. Degradation kinetics

The TiO_2 photocatalytic degradation kinetics of 6-HOMU were evaluated under 350, 420 and 450 nm irradiation for each catalyst. While TiO_2 photocatalysis is a heterogeneous process, the initial degradation kinetics often follows pseudo-first-order type kinetics [26]. The concentration of 6-HOMU was monitored by HPLC as a function of irradiation time. The plots of $\ln(C_0/C)$ as a function of treatment time exhibit linear relationships and the pseudo-first order rate constants were determined from the slope of the line. The results are summarized in Table 2.

3.3. Heterogeneous kinetics

Evaluation of reaction kinetics can provide useful mechanistic information and important parameters for the assessment and modeling TiO_2 photocatalytic treatment. TiO_2 photocatalysis involves the generation of ROS and their subsequent reactions with the adsorbed target compounds at the TiO_2 surface. In these heterogeneous processes, both adsorption and reactivity play critical roles in governing the degradation. To assess the adsorption and reactivity parameters for heterogeneous TiO_2 photocatalysis, the Langmuir–Hinshelwood (L-H) kinetic model was employed Eq. (6). The L-H model has been widely used for assessment of TiO_2 photocatalysis at the liquid–solid interfaces [26,27]. This model assumes limited surface adsorption sites, no interaction between adsorbed species on the surface and reversible adsorption reaction [28].

$$\frac{1}{r_0} = \frac{1}{k_r K C_0} + \frac{1}{k_r} \quad (6)$$

where r_0 is the initial rate, C_0 is the initial 6-HOMU concentration, k_r is a reactivity coefficient related to oxidation reactions, and K is the equilibrium constant related to surface adsorption. The L-H model applied to TiO_2 photocatalysis yields apparent kinetic parameters. The L-H experiments were conducted over a range of initial concentrations (3.52–35.2 μM) and a constant NF-TiO_2 concentration (0.1 g/L) under visible light (450 nm) irradiation (Fig. 4). The L-H kinetic parameters k_r and K were determined from the slope and

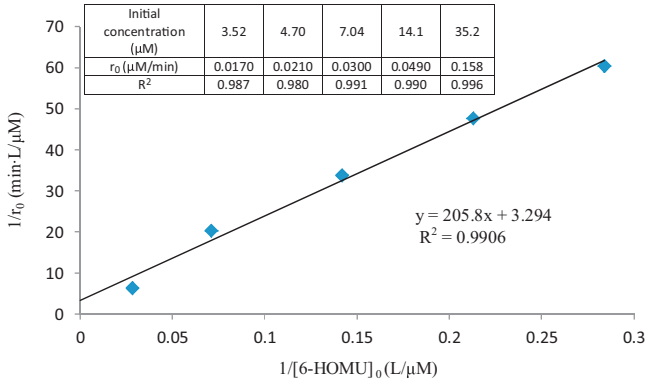

Fig. 4. L–H plot of TiO_2 photocatalysis of 6-HOMU under visible light (450 nm). The insert table is the initial rates at different concentration of 6-HOMU. [NF-TiO_2] = 0.1 g/L. The reproducibility is within ±5% on the basis of triplicate runs.

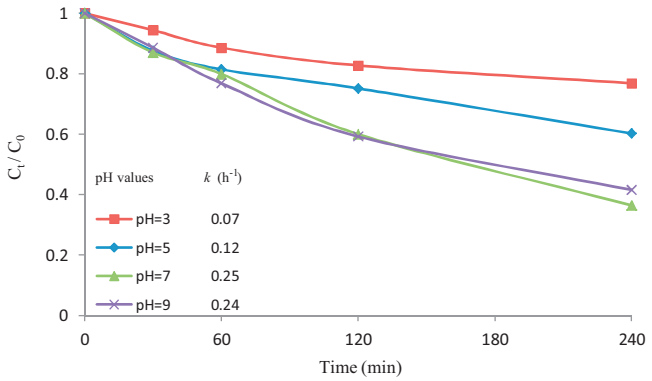

Fig. 5. TiO_2 photocatalysis of 6-HOMU at pH 3, 5, 7 and 9. The insert table is the 1st order rate constants at different solution pH. [6-HOMU]$_0$ = 1 ppm, [NF-TiO_2] = 0.1 g/L, λ = 450 nm. The reproducibility is within ±5% on the basis of triplicate runs.

intercept of the linear fit of the $1/r_0$ vs. $1/C_0$, which shows that k_r is 0.304 μM/L min and K is 0.016 L/μM under our experimental conditions. L-H kinetic parameters for phenylarsonic acid (PA) with P-25 TiO_2 using the same reaction vessels and photochemical reactor under 350 nm irradiation has been reported with k_r 2.8 μM/L min and K 0.034 L/μM [29]. The L-H parameters for PA under UV TiO_2 photocatalysis may imply stronger adsorption and a more reactive system than 6-HOMU treatment by VLA NF-TiO_2 photocatalysis. The degradations at different initial concentrations follow pseudo-first-order kinetic model (insert table in Fig. 4). The apparent kinetic parameters obtained from our results are useful for modeling and predicting specific treatment objectives.

3.4. Environmental factors on VLA TiO_2 photocatalysis

3.4.1. pH effects

VLA TiO_2 photocatalyses of 6-HOMU were performed under acidic, neutral, and basic conditions (pH 3, 5, 7 and 9). The concentrations of 6-HOMU as a function of irradiation time at different pH values are illustrated in Fig. 5. The degradation of 6-HOMU was fastest at pH 7 and 9 with overall degradation of 62 ± 3%, decreasing to 40% at pH 5 and to 23% at pH 3 after 4 h of treatment. The decrease in degradation with decreasing pH is rationalized based on electrostatic repulsion between positively charged 6-HOMU and the NF-TiO_2 surface. The point of zero charge (PZC) for NF-TiO_2 is 6.4 [17]. Under acidic conditions, the surface of NF-TiO_2 is protonated (TiO_2H^+) and possesses an overall positive charge. While the pK_a value for 6-HOMU is not reported, we assume the pK_a of 6-HOMU is similar to 5-HOMU (pK_a = 9.27) [30] and thus positively charged in the pH range of this study. The neutral and negative charges on the surface of the catalyst under neutral and basic conditions lead to stronger adsorption of the positively charged 6-HOMU and thus faster degradation. As the pH decreases the overall positive charge on the surface increases along with the electrostatic repulsion with positively charged 6-HOMU inhibiting adsorption resulting in slower degradation at under acidic conditions.

3.4.2. Dissolved metal ions effects

Dissolved ions can influence the overall efficiency of TiO_2 photocatalysis of organic compounds. In order to investigate the influence of dissolved ions on VLA TiO_2 photocatalysis, Ca^{2+}, Mg^{2+}, Fe^{3+} and Cu^{2+} ions were added to the reaction solutions in the range of 0.2–8 ppm. The effects of Ca^{2+} and Mg^{2+} ions on photocatalysis of 6-HOMU are negligible under our experimental conditions. The pseudo-first-order rate constants (k) of 6-HOMU photodegradation with Ca^{2+}, Mg^{2+} and without the ions are identical (0.25 ± 0.01 h^{-1}). The addition of Fe^{3+} and Cu^{2+} ions enhanced the VLA TiO_2

Please cite this article in press as: C. Zhao, et al., UV and visible light activated TiO_2 photocatalysis of 6-hydroxymethyl uracil, a model compound for the potent cyanotoxin cylindrospermopsin, Catal. Today (2013), http://dx.doi.org/10.1016/j.cattod.2013.09.042

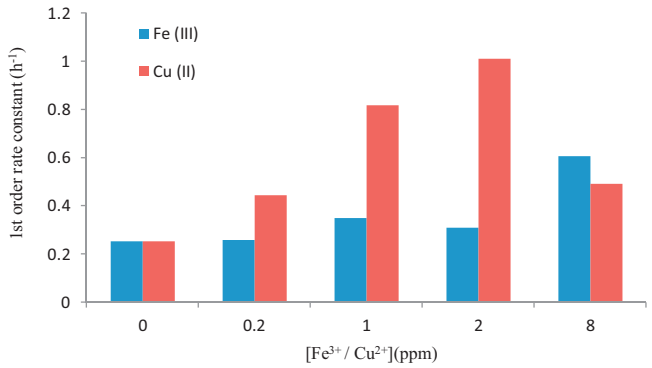

Fig. 6. The effects of Fe^{3+} and Cu^{2+} ion on TiO_2 photocatalysis of 6-HOMU. [6-HOMU]$_0$ = 1 ppm, [NF-TiO_2] = 0.1 g/L, λ = 450 nm. The reproducibility is within ±2% on the basis of triplicate runs.

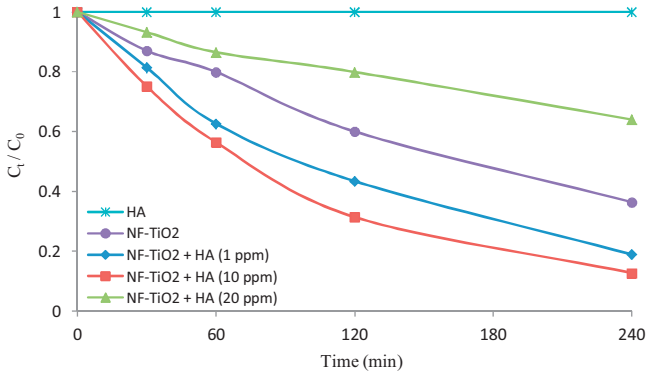

Fig. 7. The effects of HA on photo-transformation and TiO_2 photocatalysis of 6-HOMU. [6-HOMU]$_0$ = 1 ppm, [NF-TiO_2] = 0.1 g/L, λ = 450 nm. The reproducibility is within ±5% on the basis of triplicate runs.

photocatalysis of 6-HOMU. In the presence of Fe^{3+} ions, the degradation rate constant increased by ~2.5 times at a concentration of 8 ppm with pseudo-first-order rate constant (k) of 0.61 h^{-1}. The NF-TiO_2 photocatalysis process of 6-HOMU was also promoted by adding Cu^{2+} ions in the range of 0.2–2 ppm. The presence of Fe^{3+}/Fe^{2+} and Cu^{2+} ions can promote photo-Fenton/Fenton type reactions Eqs. (7) and (8) to produce HO• which may be responsible for the observed enhancement in the degradation of 6-HOMU.

$$Fe^{3+}/Cu^{2+} + e^- \rightarrow Fe^{2+}/Cu^{+} \quad (7)$$

$$Fe^{2+}/Cu^{+} + H_2O_2 \rightarrow Fe^{3+}/Cu^{2+} + HO^{\bullet} + HO^- \quad (8)$$

Fe^{3+}/Cu^{2+} ions can also scavenge the e_{cb}^- during TiO_2 photocatalysis, converting to Fe^{2+}/Cu^{+} ions, while inhibiting e_{cb}^-/h_{vb}^+ pairs recombination to indirectly increase the HO• production. The decrease in the degradation rate constant at higher Cu^{2+} ion concentrations may be the result of Cu^{2+} ions acting as the primary e_{cb}^- scavenger at the expense of dissolve oxygen, inhibiting the formation of $O_2^{\bullet-}$ and thus reducing the levels of $O_2^{\bullet-}$ and indirectly reducing the production of HO•. Under our experimental conditions, inhibition however was not observed in the case of Fe^{3+} which may be a result of stronger adsorption of Cu^{2+} at the TiO_2 surface leading to more effective competition for e_{cb}^- (Fig. 6).

3.4.3. Dissolved organic matter (DOM) effects

The presence of dissolved organic matter (DOM) can have a pronounced effect on photochemical based water treatment processes. DOM derived from decomposed biomass is composed of large carbon based structures with a number of light absorbing chromophores. Upon light absorption DOM can lead to an excited state (DOM*) Eq. (9). The DOM* can undergo energy or electron transfer pathways with molecular oxygen to generate $^1O_2$ or $O_2^{\bullet-}$ Eq. (10). These ROS can initiate the degradation of 6-HOMU, Eq. (11). The DOM* can also sensitize TiO_2 Eq. (12) leading to charge carriers with the potential to initiate degradation processes Eq. (13).

$$DOM + h\nu \rightarrow DOM* \quad (9)$$

$$DOM* + O_2 \rightarrow {}^1O_2(O_2^{\bullet-}) \quad (10)$$

$$^1O_2(O_2^{\bullet-}) + \text{6-HOMU} \rightarrow \text{6-HOMU}_{[OX]} \quad (11)$$

$$DOM* + TiO_2 \rightarrow TiO_2* \quad (12)$$

$$TiO_2* \rightarrow e_{cb}^- + h_{vb}^+ \rightarrow ROS + \text{6-HOMU} \rightarrow \text{6-HOMU}_{[OX]} \quad (13)$$

The influence of DOM on the solar photolysis of organic contaminants has been widely studied [31,32]. We used HA to assess the role of DOM* initiated degradation of 6-HOMU under 450 nm irradiation in the absence of NF-TiO_2 as a control experiment. The photolysis of 6-HOMU was also carried out in the presence of HA under 450 nm irradiation for 240 min. The concentration of 6-HOMU was monitored as a function irradiation time under different experimental conditions, shown in (Fig. 7). DOM alone did not lead to the photo-transformation 6-HOMU under our experimental conditions.

The concentrations of HA were varied from 1 to 20 ppm while holding the catalyst loading and 6-HOMU constant. The observed degradation of 6-HOMU in the absence and presence of different HA concentrations are illustrated in Fig. 7. An enhanced degradation was observed for HA concentrations between 1 and 10 ppm. This enhancement was attributed to HA photosensitized processes, in which ROS can be formed to accelerate the overall photodegradation. However, the degradation process was strongly inhibited by the increased HA because at higher concentrations, HA can act as a light filter and attenuate the photochemically active processes [33], as well as scavenge ROS leading to the reduced degradation of 6-HOMU.

3.5. The role of reactive oxygen species in VLA TiO_2 photocatalysis

UV TiO_2 photocatalysis leads to a number of ROS, among them HO• produced by h_{vb}^+ oxidation of adsorbed hydroxyl groups is generally considered responsible for the degradation of organic pollutants and toxins. While the effectiveness of UV TiO_2 photocatalysis is often correlated to the production of HO•, during VLA doped-TiO_2 photocatalysis the direct formation of HO• from h_{vb}^+ is not thermodynamically plausible. VLA doped-TiO_2 photocatalysis can however lead to the formation of HO• indirectly from $O_2^{\bullet-}$. $O_2^{\bullet-}$ can also lose an electron to produce $^1O_2$ which can contribute to the oxidation of organic compounds. In an attempt to better understand the formation and roles of different ROS during VLA NF-TiO_2 photocatalysis, specific scavengers were employed during the treatment of 6-HOMU. The degradation of 6-HOMU was carried out in the absence and presence of various quenchers and scavengers as outlined in Table 3. Molecular oxygen was used as the e_{cb}^- scavenger, t-BuOH was added as a HO• scavenger, furfuryl alcohol was used to probe the role of $^1O_2$, formic acid was used to quench oxidative processes, and superoxide dismutase employed to quench $O_2^{\bullet-}$.

The results of the quenching experiments are summarized in Fig. 8. In the absence of dissolved oxygen (Argon saturated conditions) no detectable degradation of 6-HOMU was observed during VLA NF-TiO_2 photocatalysis illustrating molecular oxygen is required for the degradation as an e_{cb}^- trap and/or in the production of $O_2^{\bullet-}$. The presence of t-BuOH, a HO• scavenger, significantly reduced the observed degradation of 6-HOMU. While hydroxyl

Please cite this article in press as: C. Zhao, et al., UV and visible light activated TiO_2 photocatalysis of 6-hydroxymethyl uracil, a model compound for the potent cyanotoxin cylindrospermopsin, Catal. Today (2013), http://dx.doi.org/10.1016/j.cattod.2013.09.042

Table 3
Scavengers effects on TiO_2 photodegradation.

Reactive species	Scavengers	Mechanisms
e_{cb}^- (electron)	O_2	$e_{cb}^- + O_2 \rightarrow O_2^{\bullet -}$ $k = 7.6 \times 10^7\ M^{-1}\ s^{-1}$ [34]
$HO^\bullet$ (hydroxyl radical)	*t*-BuOH (*tert*-Butyl alcohol)	$HO^\bullet$ + *t*-BuOH $\rightarrow H_2O + {}^\bullet CH_2C(CH_3)_2OH$ $k = 5.0 \times 10^8\ M^{-1}\ s^{-1}$ [34]
$^1O_2$ (singlet oxygen)	Furfuryl alcohol (FFA)	FFA + $^1O_2 \rightarrow FFA_{ox}$ $k = 1.2 \times 10^8\ M^{-1}\ s^{-1}$ [35]
h_{vb}^+ (hole)	HCO_2H (formic acid)	$2h_{vb}^+ + 2HCO_2^- \rightarrow CO_2 + 2H^+$
$O_2^{\bullet -}$ (superoxide anion radical)	SOD_{red} (superoxide dismutase)	$SOD_{red} + O_2^{\bullet -} + 2H^+ \rightarrow SOD + H_2O_2$ $k = 2.0 \times 10^9\ M^{-1}\ s^{-1}$ [34]

radicals do not form directly via the h_{vb}^+ oxidation of surface hydroxyl groups during VLA NF-TiO_2 photocatalysis, the formation of $HO^\bullet$ can occur indirectly via reduction of H_2O_2 the product of $O_2^{\bullet -}$ disproportion.

Furfuryl alcohol (FFA) is commonly used as a scavenger for $^1O_2$, but also readily reacts with $HO^\bullet$ [36] and thus can function as a scavenger for both $^1O_2$ and $HO^\bullet$. The decreases in degradation of 6-HOMU were similar in the presence of FFA and *t*-BuOH, a selective $HO^\bullet$ scavenger. Since FFA quenches $^1O_2$ and *t*-BuOH does not, the similar decrease in the presence of FFA or *t*-BuOH indicates $^1O_2$ plays a minimal role in the degradation process. To further test the role of $^1O_2$ in VLA NF-TiO_2 photocatalysis, the degradation of 6-HOMU was performed in D_2O. The lifetime of $^1O_2$ in D_2O is longer than that in H_2O and thus singlet oxygen mediated processes are enhanced in D_2O. The degradations in solution of H_2O and D_2O were similar indicating $^1O_2$ does not play an important role under our experimental conditions.

VLA NF-TiO_2 photocatalysis of 6-HOMU was not affected by the presence of formic acid. While formic acid has been used to quench the h_{vb}^+ mediated processes during UV TiO_2 photocatalysis, our observations are consistent with previous reports that h_{vb}^+ trapped in the region of inter-valence band does not possess the redox potential to efficiently oxidize formic acid [37]. Therefore, the produced $HO^\bullet$ in VLA NF-TiO_2 likely results from the reduction of H_2O_2 rather than oxidizing surface absorbed H_2O by h_{vb}^+. Our results indicate the photogenerated h_{vb}^+ in VLA NF-TiO_2 photocatalysis does not play a significant role in the observed degradation process.

In TiO_2 photocatalysis, dissolved oxygen serves as an electron trap and leads to the formation of $O_2^{\bullet -}$ which can proportionate or produce to $^1O_2$ with loss of an electron. In the presence of superoxide dismutase, an effective quencher of $O_2^{\bullet -}$, the degradation of 6-HOMU was completely inhibited indicating that $O_2^{\bullet -}$ is critical in the VLA NF-TiO_2 photocatalytic degradation process. $O_2^{\bullet -}$ has been implicated in the destruction of a strongly visible light absorbing dye during VLA TiO_2 photocatalysis [38]. The previous study is complicated by potential self-sensitized degradation pathways. Our model compound does not absorb visible-light and thus contributions from self-sensitized reaction pathways can be ruled out. Therefore, according to these findings, $O_2^{\bullet -}$ plays a critical role in VLA TiO_2 photocatalytic processes.

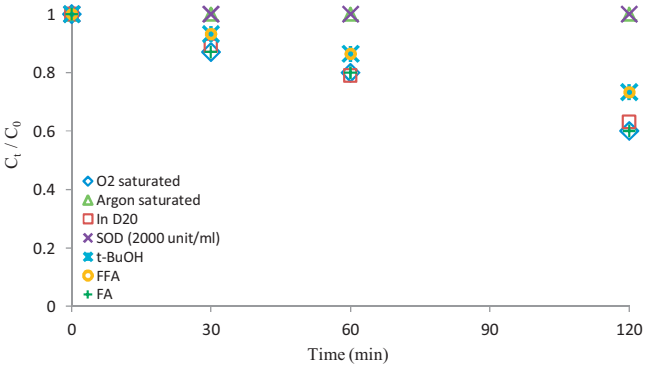

Fig. 8. The contribution of ROS to VLA TiO_2 photocatalysis. $[6\text{-HOMU}]_0 = 1$ ppm, [NF-TiO_2] = 0.1 g/L, $\lambda = 450$ nm. The reproducibility is within ±5% on the basis of triplicate runs.

4. Conclusions

S-TiO_2, PF-TiO_2 and NF-TiO_2 are photoactive under UV irradiation and the degradation of 6-HOMU follows a pseudo-first-order kinetic model. Among non-metal doped TiO_2 materials, our results indicate that NF-TiO_2 exhibits the best performance to destroy the model compound of CYN due to its high photocatalytic activity. The kinetics is accurately modeled and degradation is effective over a range of pH. A synergetic effect is observed in photodegradation of 6-HOMU in the presence of Fe^{3+}, Cu^{2+} ions and HA due to more production of $HO^\bullet$ or ROS in the photooxidation process. Experiments performed in the presence of scavengers for $O_2^{\bullet -}$, $^1O_2$, $HO^\bullet$ and h_{vb}^+ indicate that $O_2^{\bullet -}$ is the predominant species leading to the VLA TiO_2 photocatalytic destruction of 6-HOMU. Our results provide a better fundamental understanding of the different roles of ROS during VLA TiO_2 photocatalysis and demonstrate VLA TiO_2 photocatalysis has potential for water treatment for cyanotoxins.

Acknowledgement

D.D.D. and K.E.O gratefully acknowledge support from the National Science Foundation (CBET, award 1033317).

References

[1] G.A. Codd, Water Sci. Technol. 32 (1995) 149–156.
[2] L. Ho, T. Meyn, A. Keegan, D. Hoefel, J. Brookes, C.P. Saint, G. Newcombe, Water Res. 40 (2006) 768–774.
[3] A.R. Humpage, M. Fenech, P. Thomas, I.R. Falconer, Mutat. Res. Genet. Toxicol. Environ. Mutagen. 472 (2000) 155–161.
[4] A.R. Humpage, F. Fontaine, S. Froscio, P. Burcham, I.R. Falconer, J. Toxicol. Environ. Health A 68 (2005) 739–753.
[5] I.R. Falconer, A.R. Humpage, Environ. Toxicol. 16 (2001) 192–195.
[6] D.J. Griffiths, M.L. Saker, Environ. Toxicol. 18 (2003) 78–93.
[7] I. Ohtani, R.E. Moore, M.T.C. Runnegar, J. Am. Chem. Soc. 114 (1992) 7941–7942.
[8] M.L. Saker, A.D. Thomas, J.H. Norton, Environ. Toxicol. 14 (1999) 179–182.
[9] C.W.K. Chow, M. Drikas, J. House, M.D. Burch, R.M.A. Velzeboer, Water Res. 33 (1999) 3253–3262.
[10] G. Newcombe, B. Nicholson, J. Water Supply: Res. Technol. – AQUA 53 (2004) 227–239.
[11] G. Newcombe, J. Morrison, C. Hepplewhite, D.R.U. Knappe, Carbon 40 (2002) 2147–2156.
[12] E. Rodriguez, A. Sordo, J.S. Metcalf, J.L. Acero, Water Res. 41 (2007) 2048–2056.
[13] E. Rodriguez, G.D. Onstad, T.P.J. Kull, J.S. Metcalf, J.L. Acero, U. von Gunten, Water Res. 41 (2007) 3381–3393.

[14] R.S. Thakur, R. Chaudhary, C. Singh, J. Renew. Sustain. Energy 2 (2010), 042701/1–042701/37.
[15] R. Thiruvenkatachari, S. Vigneswaran, I.S. Moon, Korean J. Chem. Eng. 25 (2008) 64–72.
[16] A.Y.C. Tong, R. Braund, D.S. Warren, B.M. Peake, Central Eur. J. Chem. 10 (2012) 989–1027.
[17] M. Pelaez, A.M. de la Cruz, E. Stathatos, P. Falaras, D.D. Dionysiou, Catal. Today 144 (2009) 19–25.
[18] C. Han, M. Pelaez, V. Likodimos, A.G. Kontos, P. Falaras, K. O'Shea, D.D. Dionysiou, Appl. Catal. B 107 (2011) 77–87.
[19] J. Zhao, C. Chen, W. Ma, Top. Catal. 35 (2005) 269–278.
[20] M. Pelaez, N.T. Nolan, S.C. Pillai, M.K. Seery, P. Falaras, A.G. Kontos, P.S.M. Dunlop, J.W.J. Hamilton, J.A. Byrne, K. O'Shea, M.H. Entezari, D.D. Dionysiou, Appl. Catal. B 125 (2012) 331–349.
[21] M. Pelaez, P. Falaras, A.G. Kontos, A.M. de la Cruz, K. O'Shea, P.S.M. Dunlop, J.A. Byrne, D.D. Dionysiou, Appl. Catal. B 121–122 (2012) 30–39.
[22] W. Song, S. Yan, W.J. Cooper, D.D. Dionysiou, K.E. O'Shea, Environ. Sci. Technol. 46 (2012) 12608–12615.
[23] K.-Y. Zee-Cheng, C.-C. Cheng, J. Heterocycl. Chem. 4 (1967) 163–165.
[24] G. Wu, J. Wen, S. Nigro, A. Chen, Nanotechnology 21 (2010), 085701/1–085701/6.
[25] X. Li, H. Zhang, X. Zheng, Z. Yin, L. Wei, J. Environ. Sci. (China) 23 (2011) 1919–1924.
[26] T. Xu, Y. Cai, K.E. O'Shea, Environ. Sci. Technol. 41 (2007) 5471–5477.
[27] D.F. Ollis, J. Phys. Chem. B 109 (2005) 2439–2444.
[28] M.A. Fox, M.T. Dulay, Heterogeneous photocatalysis, Chem. Rev. 93 (1993) 341–357.
[29] S. Zheng, Y. Cai, K.E. O'Shea, J. Photochem. Photobiol. A 210 (2010) 61–68.
[30] E.J. Privat, L.C. Sowers, Mutat. Res. Fundam. Mol. Mech. Mutagen. 354 (1996) 151–156.
[31] J.J. Guerard, Y.-P. Chin, H. Mash, C.M. Hadad, Environ. Sci. Technol. 43 (2009) 8587–8592.
[32] Y. Chen, C. Hu, X. Hu, J. Qu, Environ. Sci. Technol. 43 (2009) 2760–2765.
[33] S. Canonica, U. von Gunten, J. Wenk, Environ. Sci. Technol. 45 (2011) 7947–7948.
[34] Z. Xu, C. Jing, F. Li, X. Meng, Environ. Sci. Technol. 42 (2008) 2349–2354.
[35] W.R. Haag, J. Hoigne, E. Gassman, A.M. Braun, Chemosphere 13 (1984) 631–640.
[36] A. Albinet, C. Minero, D. Vione, Sci. Total Environ. 408 (2010) 3367–3373.
[37] R. Beranek, B. Neumann, S. Sakthivel, M. Janczarek, T. Dittrich, H. Tributsch, H. Kisch, Chem. Phys. 339 (2007) 11–19.
[38] M. Stylidi, D.I. Kondarides, X.E. Verykios, Appl. Catal. B 47 (2004) 189–201.

Please cite this article in press as: C. Zhao, et al., UV and visible light activated TiO_2 photocatalysis of 6-hydroxymethyl uracil, a model compound for the potent cyanotoxin cylindrospermopsin, Catal. Today (2013), http://dx.doi.org/10.1016/j.cattod.2013.09.042